

# Search for Higgs Bosons in H to WW Decays at the Tevatron

Nils Krumnack<sup>1</sup> on behalf of the CDF and DØ Collaborations

Baylor University

**Abstract.** We present the results of searches by the CDF and DØ Collaborations for Higgs boson production in  $p\bar{p}$  collisions at  $\sqrt{s} = 1.96$  TeV. The searches are performed in the  $WW^*$  channel with  $1\text{ fb}^{-1}$  of data. In the absence of signal the results are used to set a limit on the Higgs production cross section times branching ratio.

**PACS.** 14.80.Bn Standard-model Higgs bosons – 13.85.Rm Limits on production of particles

## 1 Introduction

The Higgs boson, the last undiscovered particle of the standard model, explains the origin of mass and electroweak symmetry breaking. Within the standard model the only free parameter of the Higgs boson is its mass  $m_H$ . The combination of precision measurements indicates that its mass should be less than 144 GeV [1]. Previous direct searches at LEP have set a lower limit on the Higgs mass at 114 GeV [2]. Here we present the result of searches in the  $WW^* \rightarrow \ell\nu\ell\nu$  decay channel, which covers the whole range of allowed Higgs masses and is particularly sensitive in the high mass range.

The main signature of the  $WW^* \rightarrow \ell\nu\ell\nu$  decay channel is two leptons of opposite charge and missing transverse energy caused by the neutrinos escaping the detector undetected.

## 2 The DØ measurement

The DØ measurement uses a simple cut-based analysis [3][4]. The cuts are listed in Table 1. Control plots for the data sample are in Figure 1. To avoid the uncertainties associated with the luminosity measurement, the background is normalized to the  $Z$  mass peak which is calculated at NNLO and fitted to the observed data. The final selection variable is the  $\Delta\phi$  between the two leptons. The distribution of that variable after applying all selection cuts can be seen in Figure 2. No excess over background is observed and the data are used to set a limit on the Higgs production cross section (Figure 3).

## 3 The CDF measurement

CDF has performed two measurements in this channel, both of them using multivariate techniques. The first one uses a neural network approach [5] and the second one uses a matrix element technique [6]. These

techniques are complementary and work is being performed to integrate them into a combined limit. By construction, the matrix element method only takes leading order effects into account, while the neural network approach can also take into account next-to-leading-order effects as emulated by the parton shower models.

The neural network analysis uses the cuts in Table 2. Control plots for the event selection can be seen in Figure 4. For the events passing the cuts, a neural network is trained with the input variables in Table 2 to discriminate between signal and background. The resulting event discriminant can be seen in Figure 5. This procedure is repeated for every mass point and for each mass point a limit is calculated (Figure 6).

The basic idea of the matrix element technique is to use LO matrix elements to calculate event probabilities. For each event and process the LO matrix element is integrated over phase space:

$$P_m(\mathbf{x}) = \int \frac{d\sigma_m(\mathbf{y})}{d\mathbf{y}} \epsilon(\mathbf{y}) G(\mathbf{x}, \mathbf{y}) d\mathbf{y} \quad (1)$$

where  $\frac{d\sigma_m(\mathbf{y})}{d\mathbf{y}}$  is the matrix element,  $\epsilon(\mathbf{y})$  is the efficiency and  $G(\mathbf{x}, \mathbf{y})$  is the resolution. The matrix element analysis uses the cuts in Table 3. The data are divided into a high signal-to-background and a low signal-to-background region (see Figure 7). For each mass point a separate event discriminant is calculated and a separate limit is calculated (see Figure 8).

## 4 Combining Measurements

For each experiment the obtained limits are combined with the limits from other search channels. In addition, the limits from CDF and DØ are also combined to yield an overall Tevatron limit (see Figure 9).

**Table 1.** Cut values used in the DØ analysis.  $p_{T,i}$  is the transverse momentum of lepton  $i$  (ordered by decreasing  $p_T$ ).  $m_{l\bar{l}}$  is the invariant mass of the two-lepton system.  $\Delta\phi_{ll}$  is the difference in azimuthal angle between the two leptons.  $m_{T,\min}(l, \cancel{E}_T)$  is the minimum transverse mass of the missing transverse momentum and one of the leptons.

	ee	$e\mu$	$\mu\mu$
lepton ID	$p_{T,1} > 15, p_{T,2} > 10, m_{ll} > 15$ , isolation		
$\cancel{E}_T$	$\cancel{E}_T > 20$ , significance( $\cancel{E}_T$ ) $> 7$		
$m_{ll} < x$	$\min(m_H/2, 80)$	$m_H/2$	80
$p_{T,1} + p_{T,2} + \cancel{E}_T$	$m_H/2 + 20 < x < m_H$		$100 < x < 160$
$m_{T,\min}(l, \cancel{E}_T)$	$x > 15 + m_H/4$		$x > 55$
$H_T = \sum p_T^{\text{jet}}$	$H_T < 100$		$H_T < 70$
$\Delta\phi_{ll}$	$\Delta\phi_{ll} < 2.0$		

**Table 2.** Cut values used in the CDF neural net analysis (left) and the input variables for the neural net (right).

$p_{T,1} > 20, p_{T,2} > 10$	$p_{T,1}$	$p_{T,1} + p_{T,2} + \cancel{E}_T$
lepton isolation	$p_{T,2}$	$m_{ll}$
$m_{ll} > 16$	$n_{\text{jets}}$	$\Delta\phi_{\min}(\cancel{E}_T, \text{lepton or jet})$
$n_{\text{jet}} = 0$ or $n_{\text{jet}} = 1, E_T^{\text{jet}} < 55$ or $n_{\text{jet}} = 2, E_T^{\text{jet}} < 40$	$E_{T,1}^{\text{jet}}$	$\Delta\phi_{ll}$
opposite charge leptons	$E_{T,2}^{\text{jet}}$	$\sqrt{\Delta\eta_{ll}^2 + \Delta\phi_{ll}^2}$
neural net for Drell-Yan suppression	$\cancel{E}_T$	$\cancel{E}_T / (p_{T,1} + p_{T,2} + \cancel{E}_T)$

**Table 3.** Cut values used in the CDF matrix element analysis.

$p_{T,1} > 20, p_{T,2} > 10$
$25 < \cancel{E}_{T,rel} = \cancel{E}_T \cdot \sin(\min(\pi/2, \Delta\phi(\cancel{E}_T, \text{lepton or jet})))$
$\cancel{E}_T \sqrt{\sum E_T} > 2.5$
$n_{\text{jets}} < 2$
$m_{ll} > 25$
trilepton veto

**Fig. 1.** The invariant mass spectrum in the preselection sample for  $D\bar{O}$ . To avoid the uncertainties in the luminosity measurement, the background prediction is normalized to the  $Z$  mass peak.

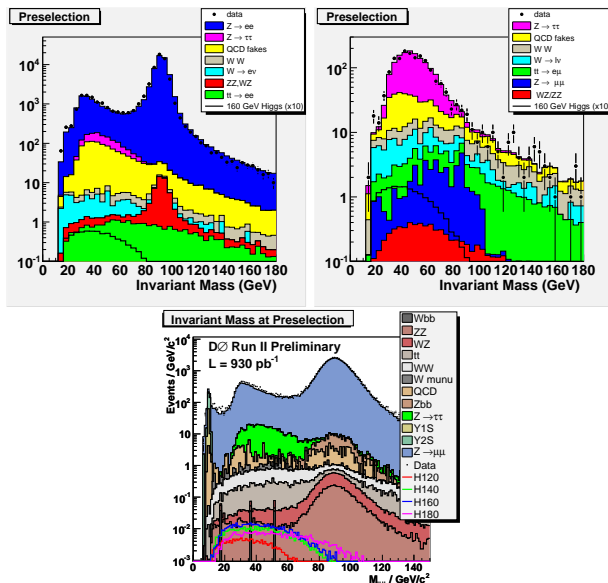
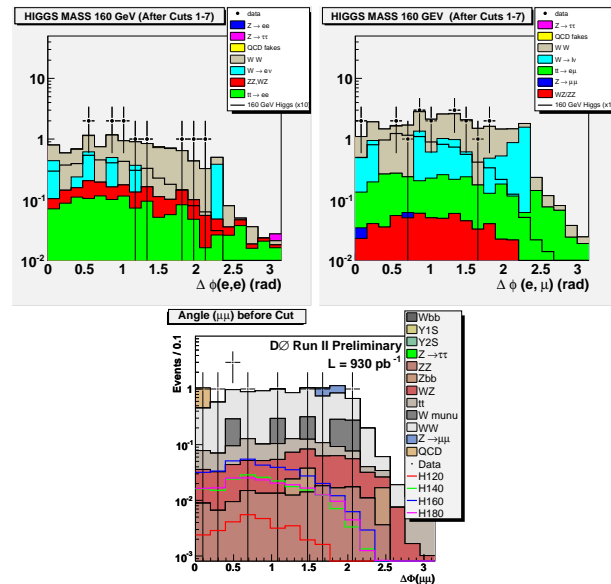


**Fig. 2.** The  $\Delta\phi$  spectrum after applying all cuts for  $D\bar{O}$ . The limit is extracted from the region  $\Delta\phi < 2$ .



## References

1. The LEP Electroweak Working Group, <http://lepewwg.web.cern.ch/LEPEWWG/>
2. R. Barate *et al.* [LEP Working Group for Higgs boson searches], Phys. Lett. B **565**, 61 (2003) [arXiv:hep-ex/0306033].
3. The DØ Collaboration, public note **DØnote 5063-CONF**, 2006
4. The DØ Collaboration, public note **DØnote 5194-CONF**, 2006
5. The CDF Collaboration, public note for cdf note **8700**, 2007

**Fig. 3.** The expected and observed  $D\bar{O}$  limit on the cross section as a function of mass. For reference the standard model cross section and the cross section for a fourth generation model are shown as well. The measurement already excludes the fourth generation model for some Higgs masses and is within a factor of 4 from the standard model prediction at 160 GeV.

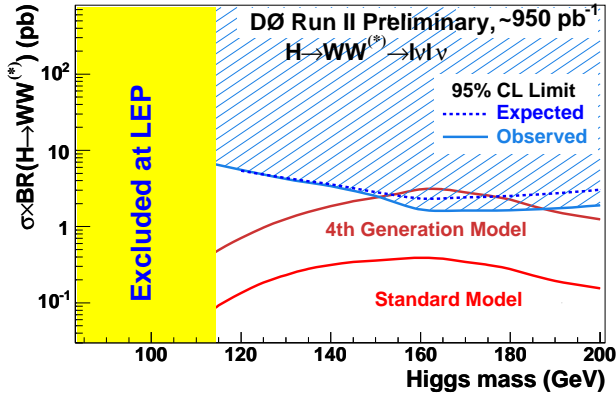


**Fig. 4.** Control plots for the CDF neural network analysis after applying the selection cuts. The background model describes the signal well and the variables allow discrimination between signal and background.

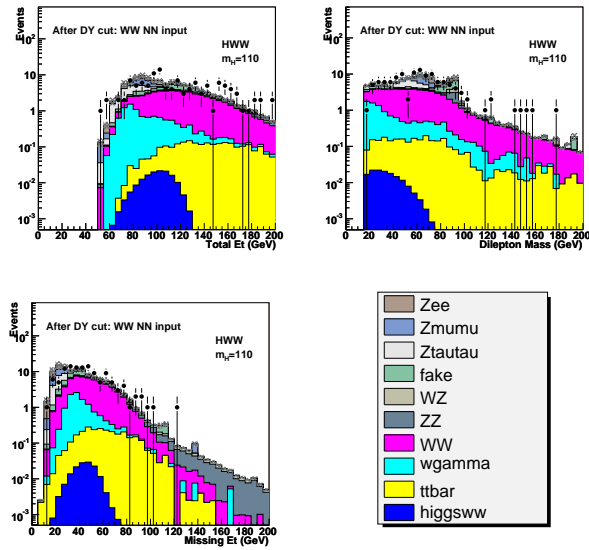


**Fig. 5.** The event discriminant (i.e. network output) for the CDF neural network analysis. The shaded area indicates the uncertainty on the background prediction. Each bin is treated as a separate counting experiment to determine the limit. A legend to the plots can be found in Figure 4.

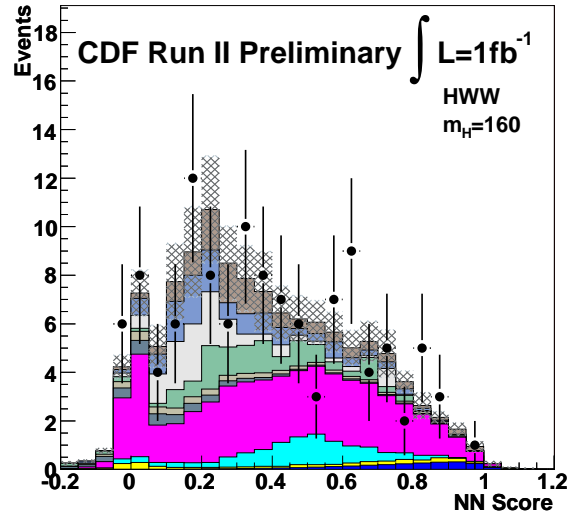


**Fig. 6.** The expected and observed cross section limit for the CDF neural network analysis. The limit is normalized to the standard model prediction. The prediction for a fourth generation model is shown as well. The measurement already excludes the fourth generation model for some Higgs masses and is within a factor of 5 from the standard model prediction at 160 GeV.

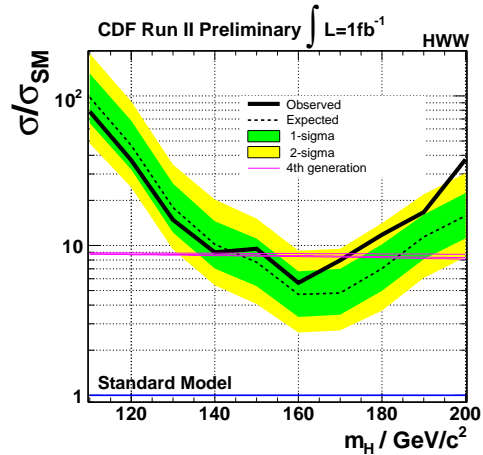


**Fig. 7.** The event discriminant for the CDF ME analysis in the low (top) and high (bottom) signal-to-background region. The inset shows a magnification of the events with high discriminant values. For comparison, the standard model Higgs prediction is shown (scaled up by a factor of 10). Each bin is treated as a separate counting experiment for the extraction of the limit.

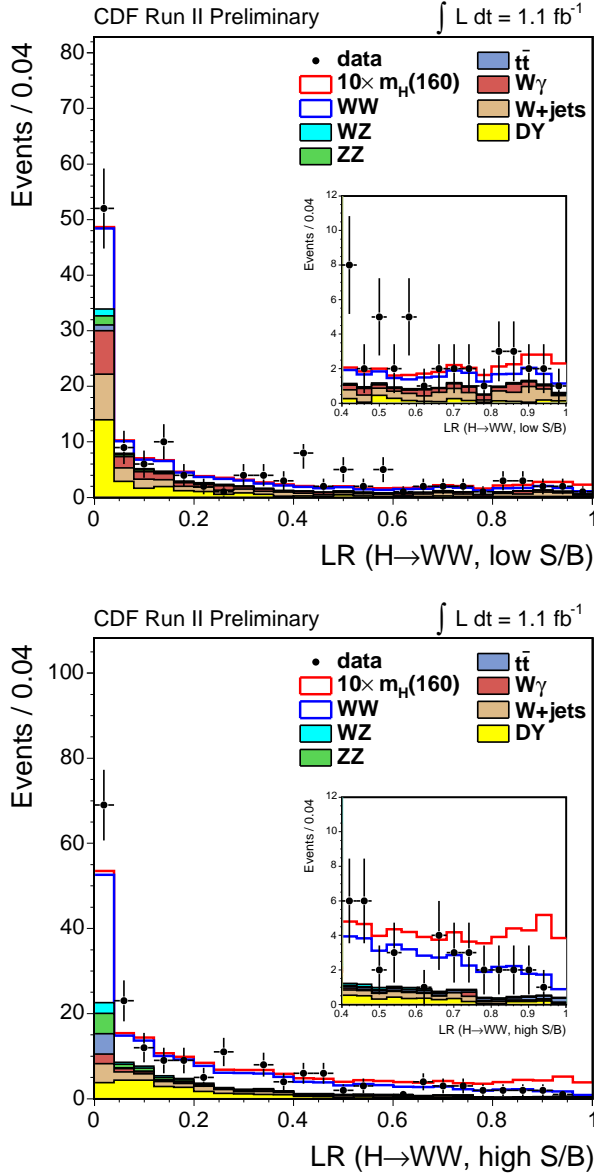


**Fig. 8.** The expected and observed cross section limit for the CDF matrix element analysis. The limit is normalized to the standard model prediction. The measurement is within a factor of 4 from the standard model prediction at 160 GeV.

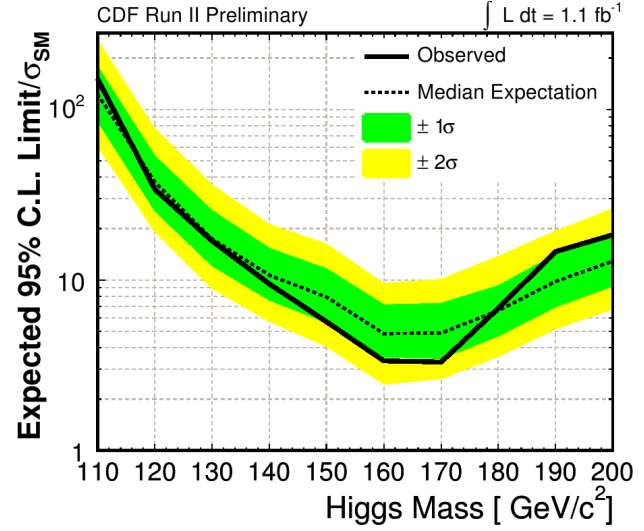


**Fig. 9.** The combined limits for both experiments and the Tevatron as a whole. The CDF combination uses an older version of the  $H \rightarrow WW$  analysis, which only used  $300 \text{ pb}^{-1}$ . Except for the low mass region the limit is dominated by the  $H \rightarrow WW$  channel and has its maximum sensitivity at 160 GeV.

